Journal of
Composites Science

MDPI

Article

Magnetic Susceptibility of a Nanocomposite Based on an Opal Matrix with $Yb_2Ti_2O_7$ Particles

Anatoly B. Rinkevich, Olga V. Nemytova * and Dmitry V. Perov

Laboratory of Quantum Nanospintronics, M. N. Miheev Institute of Metal Physics of Ural Branch of Russian Academy of Sciences, 18 Sofia Kovalevskaya Str., 620990 Ekaterinburg, Russia
* Correspondence: mif–83@mail.ru; Tel.: +7-(343)-3783697

Abstract: The DC and AC magnetic susceptibilities of an opal matrix-based nanocomposite with pyrochlore-structured ytterbium titanate particles up to 60 nm in size have been studied in the range of magnetic fields up to 30 kOe. The measurements were performed at temperatures from 2 to 200 K. The temperature dependence of the nanocomposite $Yb_2Ti_2O_7$ has been found to deviate significantly from the Curie–Weiss law. From the frequency dependence of the AC susceptibility measured in the range from 10 Hz to 10 kHz, the spin relaxation times have been determined, and two relaxation times have been found to be required for the description of the frequency dependence of the susceptibility. The field dependence of the AC susceptibility has been measured. This dependence is proved to be described by the modified Cole–Cole formula. The characteristic fields of the magnetic field dependence of the real part of the susceptibility are determined, the value of the characteristic field being found to increase with increasing temperatures.

Keywords: nanocomposites; titanates; temperature dependence of susceptibility; Curie–Weiss temperature; dynamic magnetic properties; AC susceptibility; Argand diagram

Citation: Rinkevich, A.B.; Nemytova, O.V.; Perov, D.V. Magnetic Susceptibility of a Nanocomposite Based on an Opal Matrix with $Yb_2Ti_2O_7$ Particles. *J. Compos. Sci.* **2023**, *7*, 97. https://doi.org/10.3390/jcs7030097

Academic Editor: Francesco Tornabene

Received: 25 January 2023
Revised: 10 February 2023
Accepted: 28 February 2023
Published: 3 March 2023

1. Introduction

In recent years, the magnetic properties of rare-earth titanates with the pyrochlore structure have been studied very intensively. Their chemical composition is expressed by the formula $R_2Ti_2O_7$, where R is a trivalent rare-earth metal ion. The increased interest in these compounds is due to the fact that, at low temperatures, dysprosium and holmium titanates have the properties of "spin ice"—a special frustrated magnetic state characterized by macroscopic degeneracy, that is, the same energy of states with different spin directions [1]. In a certain temperature range, $Ho_2Ti_2O_7$ and $Dy_2Ti_2O_7$ titanates are considered as spin liquids with the classical type of magnetic fluctuations. Ytterbium titanate $Yb_2Ti_2O_7$ was considered as a candidate for a material with the properties of a quantum spin liquid [2,3]. This assumption was based on experimental studies of neutron scattering, which did not reveal signs of long-range magnetic ordering [4]. Further studies proved the existence of ferromagnetic ordering at temperatures below 250 mK [5]. The problem of the ground magnetic state in $Yb_2Ti_2O_7$ has been carefully explored. These investigations have shown the complexity of the unconventional magnetic ground state and the importance of the magnetic fluctuations study. It has been found that long-range dipole–dipole interaction and short-range superexchange interaction between Yb^{3+} ions should be taken into account to describe the magnetic properties of $Yb_2Ti_2O_7$ [6]. Low-temperature magnetic ordering in ytterbium titanate has been investigated by specific heat and positive muon spin relaxation methods [7]. In [8], the presence of strong quantum fluctuations allowed one to suggest that this titanate takes a position between phases ordered ferromagnetically and antiferromagnetically.

For the results of this paper, it is important to find the ground magnetic state of $Yb_2Ti_2O_7$, since the type of the ground state affects the temperature dependence of the

magnetic susceptibility and the spin relaxation times. Thorough study by a method of neutron scattering allows one to find the ground magnetic state structure. $Yb_2Ti_2O_7$ titanate is believed to be a "splayed ferromagnet", in the structure of which the magnetic moments of the Yb^{3+} ions, located at the vertices of the tetrahedral, are directed outside this tetrahedron, in contrast to the "two spins in—two spins out" rule that is typical for "spin ice" [9–11]. The titanate passes into the ferromagnetic state through a first-order phase transition [12]. In work [13], devoted to the analysis of the conditions for the realization of the state of "quantum spin ice", a review of studies of $Yb_2Ti_2O_7$ titanate is given, and a splayed ferromagnetic structure is confirmed. The conclusion is that there is insufficient evidence that this titanate belongs to materials of the "quantum spin ice" type.

The magnetic properties of ytterbium titanate are investigated in detail in [14]. The measurement of the temperature dependence of the magnetic susceptibility of poly- and single-crystal samples allows one to determine the Curie–Weiss temperature. The magnetization curves of powder titanate are calculated and compared with the experimental results. The measured temperature dependences of several titanates, including $Yb_2Ti_2O_7$, are compared with the calculated ones based on the crystal field theory [15]. The calculation takes into account both the dipole–dipole and anisotropic superexchange interactions between the nearest rare-earth ions. The fact that the temperature dependence of the magnetic susceptibility for $Yb_2Ti_2O_7$ powder titanate does not strictly comply with the Curie–Weiss law has been found in [16].

Measurements of the AC susceptibility can provide information about the unusual magnetic properties of pyrochlore titanates [17]. To find the characteristics of exotic spin systems, the frequency behavior of the susceptibility and its high-frequency limit are important. For example, an investigation of frequency dependence of the AC susceptibility allows one to conclude that $Dy_2Ti_2O_7$ titanate, demonstrating spin ice properties, has two magnetic relaxation times [18]. One of these times, which is significant at temperatures below 2 K, is associated with a highly degenerate state of spin ice. The second relaxation time is important at the higher temperature of 10 K.

Most of the experimental studies of titanates are carried out with polycrystalline or single-crystal samples. However, titanate nanoparticles, in principle, can have specific properties. The work [19], performed on nanocomposite samples, reports that some nanocomposite titanates, including $Yb_2Ti_2O_7$, can be magnetically ordered at sufficiently high temperatures of ~10–20 K. The frequency dependence of the AC susceptibility of several nanocomposite titanates, measured in the range from 1 Hz to 10 kHz, is studied in [20]. The Cole–Cole formula [21] is used to determine magnetic relaxation times. The magnetic field dependence of the AC susceptibility of several pyrochlore titanates is explored in [22]. The dependence of the real part of the susceptibility has been found to be described by a modified formula, which is similar in structure to the Cole–Cole formula.

In this article, the temperature dependences of a nanocomposite based on an artificial opal matrix with $Yb_2Ti_2O_7$ titanium nanoparticles introduced into interspherical voids is systematically studied. The temperature dependences of susceptibility for the nanocomposite and bulk titanate samples are compared. The frequency and field dependences of the AC susceptibility are explored. The magnetic relaxation times of the nanocomposite titanate, as well as the characteristic fields for the field dependences of the AC susceptibility, are determined.

2. Materials and Methods

The crystal lattice of titanates of the $R_2Ti_2O_7$ type with the pyrochlore structure belongs to the space group $Fd-\bar{3}m$. The sublattice of rare-earth ions forms a system of tetrahedra. Figure 1 schematically shows the arrangement of rare-earth metal ions at the tetrahedron vertices. The arrows in this figure show the direction of spins in the $Yb_2Ti_2O_7$ ground state.

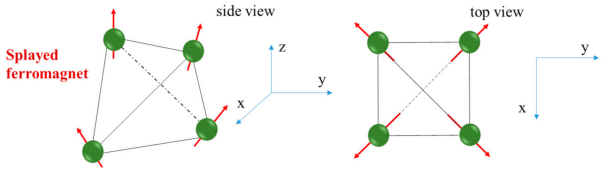

Figure 1. Schematic representation of the arrangement of spins of Yb^{3+} ions in the crystal lattice of $Yb_2Ti_2O_7$ titanate with the pyrochlore structure.

The arrangement of the spins of the Yb^{3+} ions allows for magnetic frustrated states. In accordance with the conclusions of the works [9–11], all four spins are directed outside the tetrahedron, in contrast to the direction of spins that are characteristic of frustrated pyrochlores—two inside the tetrahedron, two outside.

Opal matrices were chosen as a base for the preparation of the nanocomposites. These are structures of amorphous silicon dioxide-based submicron spheres that are from 200 to 350 nm in diameter. The choice of artificial opals is caused by the following circumstances. An empty opal matrix has a very low magnetic susceptibility [23]. Therefore, the magnetic properties of the nanocomposite are almost entirely determined by the introduced particles. A close-packed opal matrix has a periodic structure; thus, nanoparticles introduced into interspherical voids are located approximately periodically. The nanocomposite preparation technique is described in [24]. In this work, opal matrices with SiO_2 spheres that are from 240 to 280 nm in diameter were synthesized by using the following technology. The hydrolysis of orthosilicic acid ester $Si(OC_2H_5)_4$ is carried out with an ethanol solution. Ammonia hydrate is present as a catalyst. First, amorphous SiO_2 is obtained in the form of small branched nanoparticles. Later, the polycondensation process resulting in the formation of spherical-shaped amorphous SiO_2 particles takes place. After settling the suspension, a hydrogel with a liquid content of up to 60% is obtained. To increase the strength, the obtained opal matrices are subjected to heat treatment at 700 °C after drying. This procedure completely removes the rest of the water.

The simplest way to obtain nanocomposites based on an opal matrix is to impregnate the matrix with a precursor, followed by heat treatment. The precursors are usually metal nitrates with good solubility in water, which are converted into oxides at moderate heat treatment temperatures, not disturbing the shape of opal spheres and their package structure. The reaction between titanium and rare-earth oxides, which occurs during the heat treatment, is followed by the formation of pyrochlore particles. To increase the proportion of the introduced substance, the impregnation and heat treatment procedure are repeated five times. The temperature of T = 900 °C, at which the shape of silicon dioxide spheres is not distorted, is enough for the reaction of titanate obtainment. Up to a percolation threshold, the maximum size of the introduced particles is limited by the void size of ~60 nm.

The structure of the nanocomposite with the $Yb_2Ti_2O_7$ titanate nanoparticles was obtained by using an FEI Quanta-200 Pegasus scanning electron microscope at an accelerating voltage of 20 kV and a magnification of ×50,000. X-ray phase analysis was performed on a DRON-3M diffractometer in CuKα radiation, with a flat graphite monochromator. The sample was rotated either stepwise with a step of 0.02° or continuously at a rate of 1° per min.

The electrical resistance of the nanocomposites was measured. The electrical resistivity of the nanocomposites at the direct current was found to be very high, exceeding 2.5×10^7 Ω·cm. Thus, the percolation threshold was not exceeded.

Magnetic measurements were performed on a PPMS-9 setup by Quantum Design. This equipment is designed to measure physical properties such as the magnetic moment, AC susceptibility, etc. The magnetometer has static and dynamic (0.01–10,000 Hz) modes of measurement. The magnetic moment and AC susceptibility can be explored as a function of the temperature, external magnetic field, and frequency. In this work, magnetization curves were measured in the magnetic fields up to 30 kOe at the temperatures 2.5, 4, and 10 K. The temperature dependences of the magnetic moment of the sample were measured at temperatures from 2 to 200 K in fields of different strengths. The AC Measurement

System (ACMS II) utilizes a mutual induction-based technique to determine the real and imaginary parts of the dynamic (AC) susceptibility. The frequency dependences of the AC susceptibility were measured in the frequency range from 10 Hz to 10 kHz at the temperatures of 4 and 10 K. The exploration of AC susceptibility as a function of the magnetic field strength was carried out in the DC field up to 30 kOe at the temperatures of 4 and 10 K upon the magnitude of the AC magnetic field of 7 Oe, the AC magnetic field being in parallel with the DC magnetic field.

3. Results

3.1. Sample Characterization

The characterization of the nanocomposite was performed by scanning electron microscopy and X-ray phase analysis. Figure 2a shows the structure of the studied nanocomposite with the $Yb_2Ti_2O_7$ titanate nanoparticles.

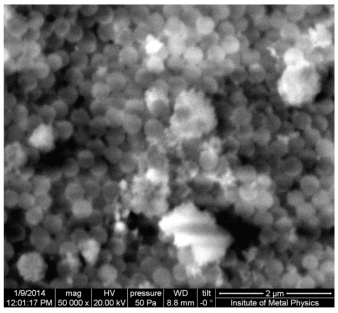

(**a**)

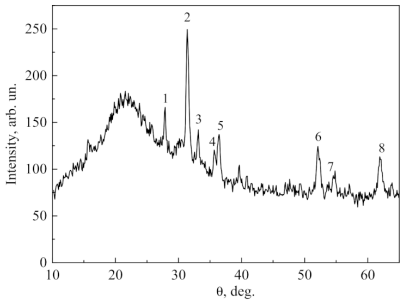

(**b**)

Figure 2. (**a**) Structure of the nanocomposite with the $Yb_2Ti_2O_7$ titanate particles, obtained by using a Quanta-200 scanning electron microscope at an accelerating voltage of 20 kV and a magnification of ×50,000; (**b**) X-ray diffraction pattern of the nanocomposite with the $Yb_2Ti_2O_7$ titanate particles.

The introduced substance is contained in the interspherical voids and partially envelops the submicron SiO_2 spheres. The particles of the ytterbium titanate in the interspherical voids have an irregular shape. Their sizes in an undamaged sample do not exceed 60 nm. The open-source Gwyddion software, version 2.56, Czech Metrology Institute, Jihlava, Czech is used to determine an average size of introduced particles, as well as to appreciate a standard deviation. As a result, the mean size of ytterbium titanate particles turned out to be 30 nm, the standard deviation being σ = 18 nm. Due to the fivefold repetition of the impregnation and heat treatment procedures, several particles may form in one void. The volume fraction of the titanate particles in the nanocomposites of about 13 ± 3 vol.% was estimated from the energy dispersive analysis data by using an EDAX instrument.

The results of the X-ray phase analysis show that the particles consist of $Yb_2Ti_2O_7$—cubic system, sp. gr. Fd − 3̄m (17-0454)—and TiO_2 (rutile)—tetragonal system, sp. gr. $P4_2/mnm$ (89–4920). Figure 2b shows the X-ray diffraction pattern of the nanocomposite. The smeared maximum near the angles 20°–22° refers to the X-ray amorphous SiO_2 matrix. The maxima in the range from 27.77° to 61.8° are due to the presence of the intro-

duced substance—ytterbium titanate and titanium oxide. The X-ray characteristics of the nanocomposite sample are given in Table 1.

Table 1. X-ray data.

No	Experimental Data					ICDD PDF-2 Data for $Yb_2Ti_2O_7$, TiO_2 (Rutile)					
	Intensity arb.un	Intensity%	Bragg Angle 2θ°	Half-Width of the Peak°	Interplanar Distance d. Å	$Yb_2Ti_2O_7$—Cubic System. sp. gr. $Fd-3m$(17-0454)			TiO_2 (Rutile)—Tetragonal Syngony. sp. gr. $P4_2/mnm$ (89-4920)		
						d. Å	hkl	I%	d. Å	hkl	I%
1	14.94	18	27.773	0.127	3.2092				3.2413	110	100
2	81.43	100	31.295	0.435	2.8556	2.8900	222	100			
3	16.57	20	32.989	0.435	2.7127						
4	12.32	15	35.618	0.429	2.5183	2.5000	400	80			
5	28.33	35	36.303	0.429	2.4723				2.4824	101	44.1
6	49.70	61	51.994	0.662	1.7571	1.7720	440	100			
7	21.40	26	54.489	0.662	1.6824	1.6940	531	40	1.6840	211	44.7
8	33.52	41	61.803	0.647	1.4997	1.5110	622	100			

3.2. Magnetic Properties

3.2.1. DC Susceptibility

The shape of the magnetization curves of the nanocomposite with the ytterbium titanate particles is typical for nanocomposites with titanate pyrochlore particles [19]. They are shown in Figure 3. Even at the low temperatures of 2–2.5 K, full magnetic saturation is not achieved, and at the temperatures above 10 K in this range of the fields, the magnetization curves are close to a linear function. In earlier studies devoted to the investigation of the magnetic properties of titanates with a pyrochlore structure, the nanocomposite based on an opal matrix with ytterbium titanate particles was shown to have a hysteresis loop, consequently having a magnetic ordering [19]. The bulk sample of the ytterbium titanate has no hysteresis and thus no signs of magnetic ordering [14,25].

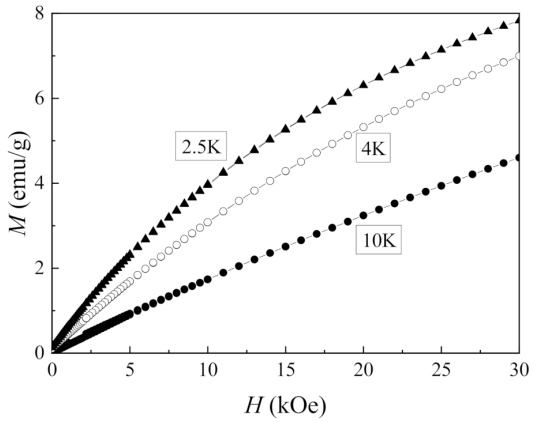

Figure 3. Magnetization curves of the nanocomposite with the ytterbium titanate particles, measured at several temperatures.

Figure 4 shows the temperature dependences of the magnetization for the nanocomposite sample, measured in fields of different strengths. These dependences are analyzed in order to determine the Curie–Weiss temperature, as well as to find the correspondence of the temperature dependences to the Curie–Weiss law. For this purpose, the temperature dependences of the inverse magnetic susceptibility are plotted. These dependences for the nanocomposite are shown in Figure 5a,b.

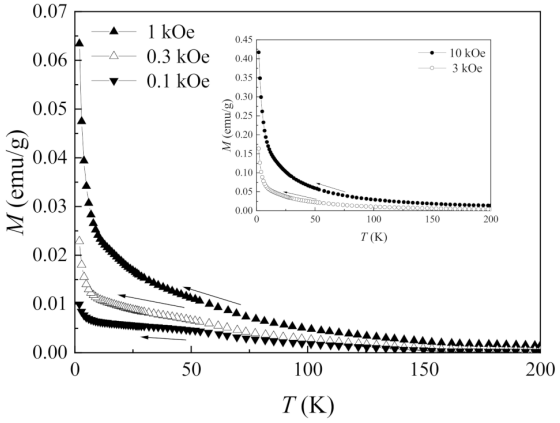

Figure 4. Temperature dependences of the magnetization for the nanocomposite sample, measured in fields of different strengths.

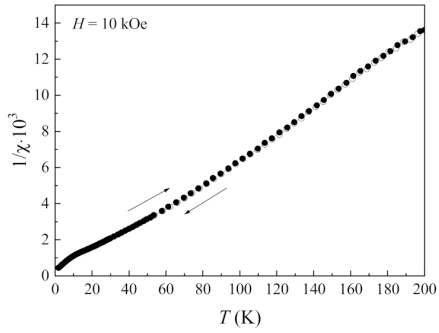

(**a**)

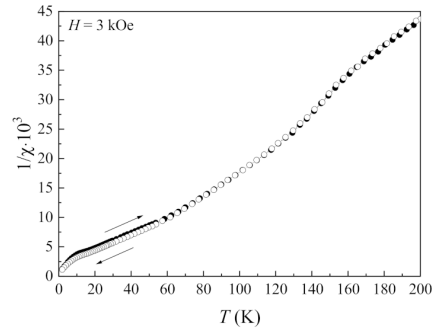

(**b**)

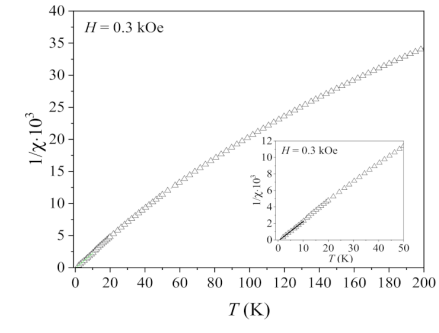

(**c**)

Figure 5. Temperature dependences of the inverse magnetic susceptibility: (**a**) for the nanocomposite sample measured in the field of 10 kOe; (**b**) for the nanocomposite sample measured in the field of 3 kOe; (**c**) for the bulk sample measured in the field of 0.3 kOe.

Figure 5c shows the temperature dependence of the inverse susceptibility for the bulk sample pressed from ytterbium titanate powder. One can see that the Curie–Weiss law for the bulk titanate is approximately fulfilled in the temperature range from 2 to 12 K. The Curie–Weiss temperature value, $\theta_{CW} \approx 0.7$ K, is comparable to the one known from the literature [14]. In contrast to the bulk titanate, for nanocomposite samples, there are very pronounced deviations from the Curie–Weiss law, even upon measurements in fairly strong fields of 10 kOe (Figure 5a) and 3 kOe (Figure 5b). The dependences measured during cooling and heating almost coincide, so there is no temperature hysteresis in the susceptibility.

3.2.2. AC Susceptibility (Frequency Dependence)

The frequency dependences of the AC susceptibility were examined in order to study the dispersion of the susceptibility and subsequently determine the magnetic relaxation times. These dependences were measured in the range from 10 Hz to 10 kHz at the AC magnetic field amplitude of 7 Oe.

The dependences of the real part of the susceptibility, measured at the temperatures 4 and 10 K, are shown in Figure 6a. The susceptibility dispersion is seen to be more pronounced for low frequencies $f < 100$ Hz. Figure 6b shows the variation in the real and imaginary parts of the AC susceptibility at $T = 4$ K. While increasing the frequency, the real part of the susceptibility χ' decreases, and the imaginary χ'' has a maximum; after that, it decreases. Figure 7 shows the Argand diagram, i.e., the dependence $\chi''(\chi')$ obtained upon the frequency variation.

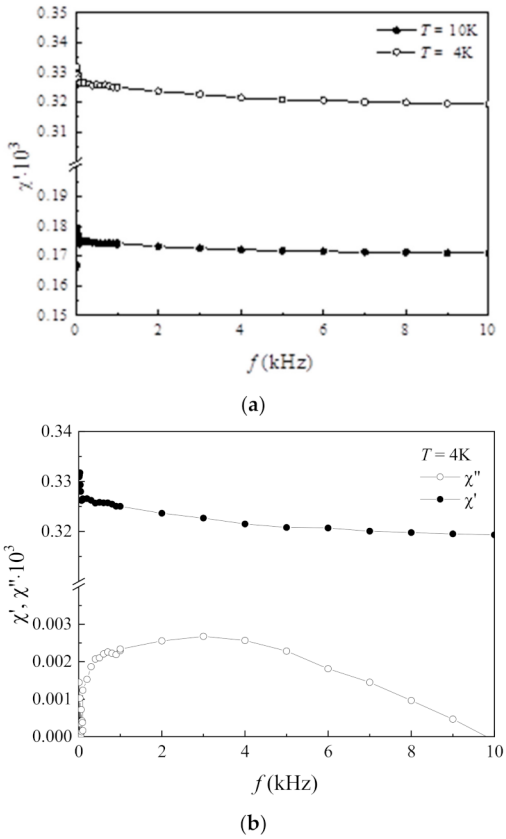

Figure 6. Frequency dependences of the AC susceptibility for the composite: (**a**) measurement of the real part of the susceptibility at 4 and 10 K; (**b**) measurement of the real and imaginary parts of the susceptibility at 4 K.

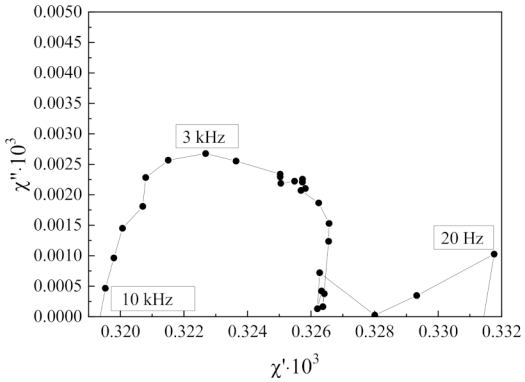

Figure 7. Argand diagram plotted at T = 4 K for the AC susceptibility of the composite with the ytterbium titanate particles.

3.2.3. AC Susceptibility (Field Dependence)

In addition to the frequency dependences, the magnetic field dependences of the AC susceptibility were measured. The measurement results at the frequencies of 10 Hz and 10 kHz at the temperatures 4 and 10 K are shown in Figure 8. While increasing the magnetic field strength, χ' is seen to decrease.

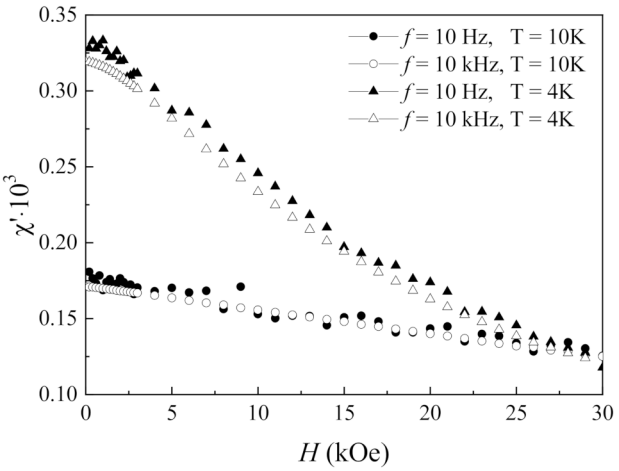

Figure 8. Magnetic field dependences of the real part of the AC susceptibility for the nanocomposite with the ytterbium particles.

4. Discussion

The temperature dependence of the bulk powder samples of ytterbium titanate is explored in [14]. There, the Curie–Weiss law was found to be fulfilled very accurately in the temperature range from 3 to 12 K. Below 3 K, there is a slight deviation from the Curie–Weiss law. The Curie–Weiss temperature turned out to be $\theta_{CW} \approx 0.8$ K, which is comparable to our results on the powder-pressed bulk sample. The temperature dependence of the magnetic susceptibility for the powder-pressed $Yb_2Ti_2O_7$ is analyzed in [16]. In this work, several models with an anisotropic tensor g and isotropic/anisotropic interionic coupling are considered. The model with anisotropic interionic coupling is turned out to fit better with the experimental data. In [6], the temperature dependence of the product $\chi \cdot T$ is analyzed. In this titanate, the superexchange between the nearest Yb^{3+} ions is concluded to predominate over the magnetic dipole interaction. Note that for bulk powder samples in a wider temperature range up to 300 K, a significant deviation from the Curie–Weiss law is recorded [25,26].

Our data on the temperature dependence of the magnetic susceptibility of the nanocomposite ytterbium titanate indicate a very significant deviation from the Curie–Weiss law. We exclude an influence of an opal matrix on the run of temperature dependence, since the magnetic susceptibility of an empty opal matrix is shown not to exceed 7×10^{-7} cm^3/g. It

is possible that these deviations are related to the magnetic ordering of the nanocomposite ytterbium titanate found in [19]. While changing the temperature, in particular, such a characteristic of the magnetic state as the coercive force changes.

Let us now discuss the results of the measurement of the AC susceptibility. The frequency dependence of the complex AC susceptibility is considered in the Cole–Cole model, in which the response of the system is described by oscillations of a system of oscillators [21]. For a system of K oscillators, the frequency distribution of oscillators with average frequencies$\nu_k = 1/\tau_k$, where τ_k is the spin relaxation time associated with the kth oscillator and the relative width of the frequency distribution α_k, is introduced. The frequency dependence $\dot{\chi}(\omega)$ is calculated by Formula (1):

$$\dot{\chi}(\omega) = \sum_{k=1}^{K} \left(\chi_k^{\infty} + \frac{\chi_k^0 - \chi_k^{\infty}}{1 + (i\omega\tau_k)^{1-\alpha_k}} \right) 0 \le \alpha_k < 1, \quad (1)$$

where $\omega = 2\pi f$ is the angular frequency, χ_k^0 is the magnetic susceptibility at $\omega \to 0$, χ_k^{∞} is the adiabatic magnetic susceptibility in the high-frequency limit. In the case of one oscillator, and upon $\alpha_k = 0$, the Debye formula is obtained. In this case, the diagram that is expressive of the dependence of $\chi''(\chi')$ looks like a semicircle.

The measurement results of the frequency dependence of the AC susceptibility shown in Figure 6 are approximated using Formula (1). This procedure is the least mean square data fitting by varying the parameter sets χ_k^0, χ_k^{∞}, α_k, and τ_k, when K equals 1 or 2. The results of the fitting are given in Figure 9. The two-relaxation-times model describes the experimental data more exactly than the one-relaxation-time model.

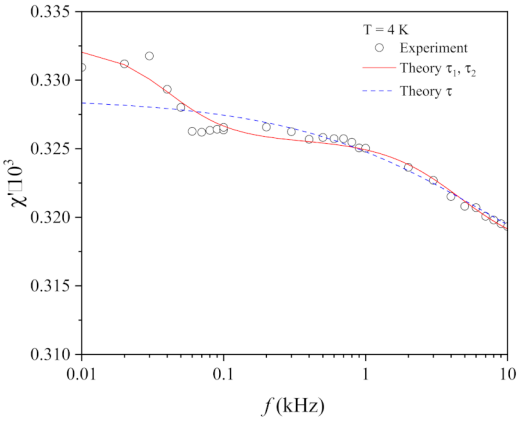

Figure 9. Results of the fitting of the frequency dependency of dynamic AC susceptibility for the nanocomposite with the ytterbium particles.

Therefore, two spin relaxation times are found to be required to describe the system response. At the temperature of 4 K, these values are equal: $\tau_1 = 3.44 \times 10^{-5}$ s and $\tau_2 = 3.85 \times 10^{-3}$ s, in accordance with the results of [20]. Similarly, at the temperature of 10 K, these values are $\tau_1 = 3.60 \times 10^{-5}$ s and $\tau_2 = 3.65 \times 10^{-3}$ s. Therefore, two relaxation times are shown to be required to describe the frequency dependence of the susceptibility at the temperatures of 4 K and 10 K. These relaxation times, determined at such high temperatures, are assumed to be in no way related to the spin ice state. The parameters α_k for the nanocomposite ytterbium titanate have the values $\alpha_k << 1$, so two harmonic oscillators with a narrow frequency spectrum are enough to describe the frequency dependence.

Figure 10 shows the $\chi''(\chi')$ dependence on which the experimental data from Figure 7 are marked with symbols, and two semicircles with the centers on the abscissa axis at the points $\chi'_{01} = 0.3227$ and $\chi'_{02} = 0.331$ are plotted. Of course, the representation of the $\chi''(\chi')$ dependence in the view of two semicircles is only qualitatively similar to the experimental data. This is especially true for the measured data at the low frequencies. They can be

obtained with an error because the mass of the introduced substance in the nanocomposite is small. Figure 10 proves that it is not enough to use Formula (1) with one oscillator to describe the frequency dependence of the AC susceptibility of the composite with the $Yb_2Ti_2O_7$ particles. At the same time, an approximate description in a model with at least two oscillators is possible.

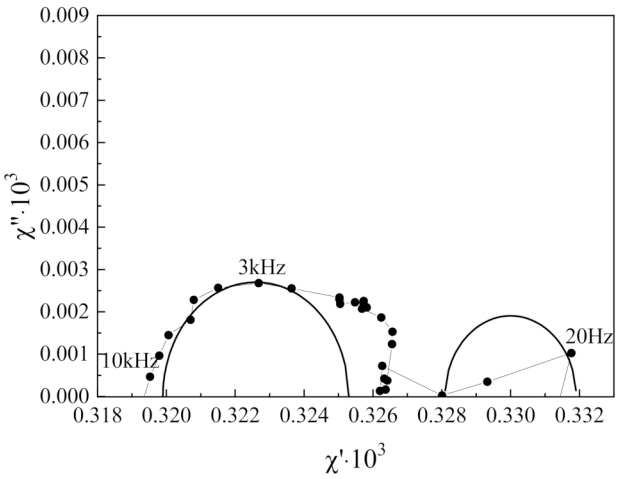

Figure 10. Argand diagram for the $\chi''(\chi')$ dependence. Symbols are the experiment; semicircles are the calculation. The centers of the semicircles are at the points with the coordinates (0.3227; 0) and (0.331; 0).

To describe the field dependences of the AC susceptibility for the rare-earth titanates, a modified Cole–Cole formula that is similar in structure to Formula (1) is proposed in [22]:

$$\chi(H) = \chi'(H) - i\chi''(H) = \chi_\infty + \frac{\chi_0 - \chi_\infty}{1 + \left(i\frac{H}{H_r}\right)^{1-\alpha}}, \quad (2)$$

where χ_0 is the AC susceptibility at $H \to 0$, and χ_∞ is the AC susceptibility at $H \to \infty$. The difference $\chi_0 - \chi_\infty$ determines the variation in the complex susceptibility in the magnetic field. In (2), a certain characteristic field of the field dependence of the susceptibility H_r is introduced. The physical meaning of the field H_r is as follows. At $\alpha = 0$, the real part of the susceptibility, which depends on the magnetic field, decreases by a factor of two compared to the value at $H = 0$. From Formula (2), for the field dependence of the real part of the AC susceptibility, one can obtain

$$\chi' = \frac{\chi_0\left(1 + \left|\frac{H}{H_r}\right|^{1-a}\cos\left(\frac{\pi}{2}(1-a)\right)\right)}{D_x}, \quad (3)$$

where

$$D_x = \left(1 + \left|\frac{H}{H_r}\right|^{1-a}\cos\left(\frac{\pi}{2}(1-a)\right)\right)^2 + \left(\left|\frac{H}{H_r}\right|^{1-a}\sin\left(\frac{\pi}{2}(1-a)\mathrm{sgn}\left(\frac{H}{H_r}\right)\right)\right)^2.$$

Upon $\alpha = 0$, Formula (3) is simplified:

$$\chi' = \frac{\chi_0}{1 + \left(\frac{H}{H_r}\right)^2}, \quad (4)$$

In [22], Formulas (3) and (4) are found to describe a field dependence of the real part of the AC susceptibility of several nanocomposite rare-earth titanates—in particular, those with $Gd_2Ti_2O_7$, $Yb_2Ti_2O_7$, $Dy_2Ti_2O_7$, Dy_2TiSiO_7, $Er_2Ti_2O_7$, and $Sm_2Ti_2O_7$ particles. In [22], composites with $Gd_2Ti_2O_7$, $Dy_2Ti_2O_7$, and Dy_2TiSiO_7 particles are studied in most detail. In this work, an approximation by Formula (2) for the nanocomposite with $Yb_2Ti_2O_7$

particles will be performed. Let us consider the experimental results for the frequency of f = 10 kHz, shown in Figure 8. Figure 11 shows their approximation by Formula (3). The approximated dependences are seen to match exactly with the experimental data. At the temperature T = 4 K, the value of the field H_r turned out to be 17 kOe, and at the temperature T = 10 K, H_r = 64 kOe. The trend of increasing the characteristic field H_r while increasing the temperature, noted in [22], is confirmed in our study of the nanocomposite with the $Yb_2Ti_2O_7$ particles.

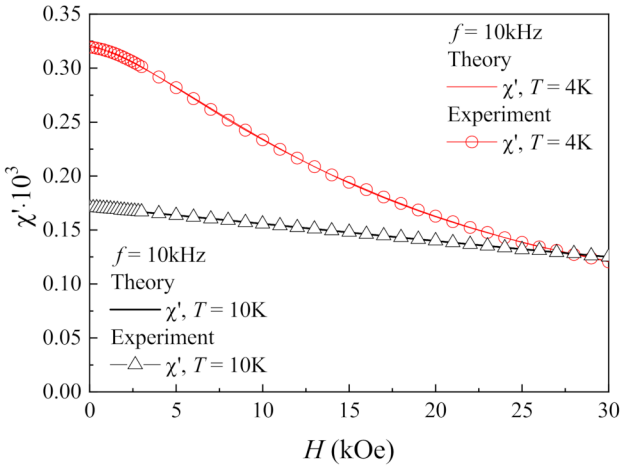

Figure 11. Approximation of the field dependences of the real part of the AC susceptibility of the nanocomposite titanate with the $Yb_2Ti_2O_7$ particles, measured at the frequency f = 10 kHz at the temperatures T = 4 K and 10 K.

5. Conclusions

The magnetic properties of the nanocomposite with $Yb_2Ti_2O_7$ titanate particles with the pyrochlore structure have been investigated. The nanocomposite is prepared based on the artificial opal matrix with the introduced titanate particles. The magnetization curves and temperature dependences of the magnetization have been measured for the different values of the magnetic field strength. The temperature dependence of the nanocomposite susceptibility has been shown not to satisfy the Curie–Weiss law. At temperatures below 150 K, significant deviation from the Curie–Weiss law is observed. The probable reason for the deviations from this law is concerned with the magnetic ordering in the nanocomposite samples.

The AC susceptibility of the nanocomposite has been explored in the frequency range from 10 Hz to 10 kHz. The frequency dependence of the real part of the complex magnetic susceptibility has been found to satisfy a model consisting of two oscillators with two relaxation times, since the one-relaxation-time model fairly describes the experimentally obtained frequency dependences of the AC susceptibility only in the frequency range from 800 Hz to 10,000Hz, whereas the two-relaxation-time model effectively describes these dependences in the whole chosen frequency range from 10 Hz to 10 kHz. The spin relaxation times corresponding to these oscillators have been determined. The fact that, at T = 4 and 10 K, two relaxation times are required to describe the frequency dependence of the AC susceptibility indicates that these relaxation processes are not related to the spin ice state. In the fields up to 30 kOe, the magnetic field dependence of the real part of the complex magnetic susceptibility of the nanocomposite has been measured. The field dependence of the AC susceptibility has been found to be described by the modified Cole–Cole formula. The characteristic field H_r, upon which the real part of the susceptibility decreases by a factor of two compared to the value at H = 0, has been calculated. At the temperature T = 4 K, the value of the field H_r turned out to be 17 kOe, and at the temperature T = 10 K, H_r = 64 kOe. Therefore, the characteristic field of this dependence increases while the temperature increases.

In general, considering the run of the magnetization curves, the temperature dependences of the DC susceptibility, and the frequency dependence of the AC susceptibility, we can conclude that the studied magnetic properties of the nanocomposite ytterbium titanate do not provide arguments in favor of the existence of quantum spin ice in this composite at low temperatures. Taking into account the results of [19], they are rather consistent with the idea of a nanocomposite in which magnetic ordering close to ferromagnetic ordering is realized.

Author Contributions: Conceptualization, A.B.R.; methodology, A.B.R. and O.V.N.; validation, A.B.R. and O.V.N.; investigation, A.B.R., D.V.P. and O.V.N.; writing—original draft preparation, A.B.R.; writing—review and editing, A.B.R., D.V.P. and O.V.N. All authors have read and agreed to the published version of the manuscript.

Funding: This research was funded by the Ministry of Science and Education of Russia (themes "Spin" No 122021000036-3 and "Function" No 122021000035-6).

Acknowledgments: The magnetic measurements were carried out with a PPMS-9 magnetometer at the Collaborative Access Center "Testing Center of Nanotechnology and Advanced Materials" of the IMP UB RAS. The authors are grateful to A.V. Korolev for the helpful comments and magnetic measurements.

Conflicts of Interest: The authors declare no conflict of interest.

References

1. Bramwell, S.T.; Gingras, M.J.P. Spin Ice State in Frustrated Magnetic Pyrochlore Materials. *Science* **2001**, *294*, 1495–1501. [CrossRef] [PubMed]
2. Applegate, R.; Hayre, N.R.; Singh, R.R.P.; Lin, T.; Day, A.G.R.; Gingras, M.J.P. Vindication of $Yb_2Ti_2O_7$ as a Model Exchange Quantum Spin Ice. *Phys. Rev. Lett.* **2012**, *109*, 097205. [CrossRef] [PubMed]
3. Ross, K.A.; Savary, L.; Gaulin, B.D.; Balents, L. Quantum Excitations in Quantum Spin Ice. *Phys. Rev. X* **2011**, *1*, 021002. [CrossRef]
4. Hodges, J.A.; Bonville, P.; Forget, A.; Yaouanc, A.; Dalmas de Reotier, P.; Andre, G.; Rams, M.; Krolas, K.; Ritter, C.; Gubbens, P.C.M.; et al. First-Order Transition in the Spin Dynamics of Geometrically Frustrated $Yb_2Ti_2O_7$. *Phys. Rev. Lett.* **2002**, *88*, 077204. [CrossRef] [PubMed]
5. Dun, Z.L.; Lee, M.; Choi, E.S.; Hallas, A.M.; Wiebe, C.R.; Gardner, J.S.; Arrighi, E.; Freitas, R.S.; Arevalo-Lopez, A.M.; Attfield, J.P.; et al. Chemical pressure effects on magnetism in the quantum spin liquid candidates $Yb_2X_2O_7$ (X = Sn, Ti, Ge). *Phys. Rev. B* **2014**, *89*, 064401. [CrossRef]
6. Siddharthan, R.; Shastry, B.S.; Ramirez, A.P.; Hayashi, A.; Cava, R.J.; Rosenkranz, S. Ising Pyrochlore Magnets: Low-Temperature Properties, "Ice Rules", and Beyond. *Phys. Rev. Lett.* **1999**, *83*, 1854–1857. [CrossRef]
7. D'Ortenzio, R.M.; Dabkowska, H.A.; Dunsiger, S.R.; Gaulin, B.D.; Gingras, M.J.P.; Goko, T.; Kycia, J.B.; Liu, L.; Medina, T.; Munsie, T.J.; et al. Unconventional magnetic ground state in $Yb_2Ti_2O_7$. *Phys. Rev. B* **2013**, *88*, 134428. [CrossRef]
8. Robert, J.; Lhotel, E.; Remenyi, G.; Sahling, S.; Mirebeau, I.; Decorse, C.; Canals, B.; Petit, S. Spin dynamics in the presence of competing ferromagnetic and antiferromagnetic correlations in $Yb_2Ti_2O_7$. *Phys. Rev. B* **2015**, *92*, 064425. [CrossRef]
9. Yaouanc, A.; Dalmas de Réotier, P.; Keller, L.; Roessli, B.; Forget, A. A novel type of splayed ferromagnetic order observed in $Yb_2Ti_2O_7$. *J. Phys. Condens. Matter* **2016**, *28*, 426002. [CrossRef]
10. Kermarrec, E.; Gaudet, J.; Fritsch, K.; Khasanov, R.; Guguchia, Z.; Ritter, C.; Ross, K.A.; Dabkowska, H.A.; Gaulin, B.D. Ground state selection under pressure in the quantum pyrochlore magnet $Yb_2Ti_2O_7$. *Nat. Commun.* **2017**, *8*, 14810. [CrossRef]
11. Gaudet, J.; Ross, K.A.; Kermarrec, E.; Butch, N.P.; Ehlers, G.; Dabkowska, H.A.; Gaulin, B.D. Gapless quantum excitations from an icelike splayed ferromagnetic ground state in stoichiometric $Yb_2Ti_2O_7$. *Phys. Rev. B* **2016**, *93*, 064406. [CrossRef]
12. Chang, L.-J.; Onoda, S.; Su, Y.; Kao, Y.-J.; Tsuei, K.-D.; Yasui, Y.; Kakurai, K.; Lees, M.R. Higgs transition from a magnetic Coulomb liquid to a ferromagnet in $Yb_2Ti_2O_7$. *Nat. Commun.* **2012**, *3*, 992. [CrossRef] [PubMed]
13. Gingras, M.J.P.; McClarty, P.A. Quantum spin ice: A search for gapless quantum spin liquids in pyrochlore magnets. *Rep. Prog. Phys.* **2014**, *77*, 056501. [CrossRef] [PubMed]
14. Hodges, J.A.; Bonville, P.; Forget, A.; Rams, M.; Kr'olas, K.; Dhalenne, G. The crystal field and exchange interactions in $Yb_2Ti_2O_7$. *J. Phys. Condens. Matter* **2001**, *13*, 9301–9310. [CrossRef]
15. Malkin, B.Z.; Lummen, T.T.A.; van Loosdrecht, P.H.M.; Dhalenne, G.; Zakirov, A.R. Static magnetic susceptibility, crystal field and exchange interactions in rare earth titanate pyrochlores. *J. Phys. Condens. Matter* **2010**, *22*, 276003. [CrossRef]
16. Cao, H.B.; Gukasov, A.; Mirebeau, I.; Bonville, P. Anisotropic exchange in frustrated pyrochlore $Yb_2Ti_2O_7$. *J. Phys. Condens. Matter* **2009**, *21*, 492202. [CrossRef]
17. Bovo, L.; Bloxsom, J.A.; Prabhakaran, D.; Aeppli, G.; Bramwell, S.T. Brownian motion and quantum dynamics of magnetic monopoles in spin ice. *Nat. Commun.* **2013**, *4*, 1535. [CrossRef]
18. Matsuhira, K.; Hinatsu, Y.; Sakakibara, T. Novel dynamical magnetic properties in the spin ice compound $Dy_2Ti_2O_7$. *J. Phys. Condens. Matter* **2001**, *13*, L737–L746. [CrossRef]

19. Rinkevich, A.B.; Korolev, A.V.; Samoylovich, M.I.; Demokritov, S.O.; Perov, D.V. Plateau on temperature dependence of magnetization of nanostructured rare earth titanates. *J. Magn. Magn. Mater.* **2018**, *453*, 137–141. [CrossRef]
20. Rinkevich, A.B.; Perov, D.V. Magnetic Susceptibility of Nanocomposite Rare-Earth Titanates in Alternating Fields. *Phys. Solid State* **2020**, *62*, 2325–2331. [CrossRef]
21. Cole, K.S.; Cole, R.H. Dispersion and absorption in dielectrics. I. Alternating current. *J. Chem. Phys.* **1941**, *9*, 341. [CrossRef]
22. Rinkevich, A.B.; Perov., D.V. Cole-Cole formula for dependence of dynamic magnetic susceptibility of rare-earth titanates on magnetic field. *J. Magn. Magn. Mater.* **2021**, *530*, 167917. [CrossRef]
23. Ávila-Crisóstomo, C.E.; Pal, U.; Pérez-Rodríguez, F.; Shelyapina, M.G.; Shmyreva, A.A. Local-field effect on the hybrid ferromagnetic-diamagnetic response of opals with Ni nanoparticles. *J. Magn. Magn. Mater.* **2020**, *514*, 167102. [CrossRef]
24. Rinkevich, A.B.; Burkhanov, A.M.; Samoilovich, M.I.; Belyanin, A.F.; Kleshcheva, S.M.; Kuznetsov, E.A. Three-Dimensional Nanocomposite Metal Dielectric Materials on the Basis of Opal Matrices. *Rus. J. Gen. Chem.* **2013**, *83*, 2148–2158. [CrossRef]
25. Rinkevich, A.B.; Koroleva, M.V.; Piir, I.V.; Perov, D.V. Magnetic Properties of Bismuth-Doped Ytterbium and Holmium Pyrochlore Titanates. *Phys. Solid State* **2019**, *61*, 1401–1408. [CrossRef]
26. Ross, K.A.; Proffen, T.; Dabkowska, H.A.; Quilliam, J.A.; Yaraskavitch, L.R.; Kycia, J.B.; Gaulin, B.D. Lightly stuffed pyrochlore structure of single-crystalline $Yb_2Ti_2O_7$ grown by the optical floating zone technique. *Phys. Rev. B* **2012**, *86*, 174424. [CrossRef]